ORBIT ANALYSYS AND MAGNET DESIGN OF TARN II

A. Noda, M. Kanazawa, T. Katayama, M. Kodaira, M. Mutou,
N. Takahashi, T. Tanabe, H. Tsujikawa and A. Mizobuchi
Institute for Nuclear Study, University of Tokyo
Midori-cho 3-2-1, Tanashi-city, Tokyo 188, Japan

A. Itano and M. Takanaka
National Institute of Radiological Sciences
Anagawa 4-9-1, Chiba-city, Chiba 260, Japan

Abstract

As the improvement project of TARN, a ring with radius of ∿ 12 m (TARN II) is designed. It can accelerate ions with ε of 1/2 up to 450 MeV/u and proton up to 1300 MeV. Further it is designed to be operated also as a cooler ring which utilize stochastic and electron cooling to realize high quality beam.

Dipole magnets with AC characteristics for the ring have already been fabricated with H-type, which is found to have realized the required good field region of ±100 mm from the result of static field measurement.

Introduction

At TARN (Test Accumulation Ring for NUMATRON project), a lot of accelerator developments have been studied[1]. For example, combination of multi-turn injection into transverse phase space and RF-stacking into longitudinal phase space has attained intensity multiplication as large as ∿300 times and recently the momentum spread of the stacked beam has been successfully reduced by stochastic cooling with Notch Filter method.

However due to DC characteristics of the dipole magnets in TARN, development related to synchrotron acceleration is out of scope of TARN and its rather limited length of straight section (1.8 m) prevents us from installation of equipments for beam extraction or electron cooling.

On the other hand, the necessity of heavy ion synchrotron such as NUMATRON[2] has been increasing more and more in recent years not only for nuclear physics but also for other applications as medical use and cooler rings which utilize electron and/or stochastic cooling have been proposed at many institutes all over the world and some of them are already under construction.

Considering such situation, TARN is decided to be improved to the larger one (TARN II). Its mean radius is almost twice as large as TARN (∿12 m) and it is designed to be able to accelerate proton up to 1300 MeV and ions with ε(charge to mass ratio) of 1/2 up to 450 MeV/u.

As the injector of TARN II , the SF cyclotron at INS is considered for the time being. Layout of TARN II is shown in Fig. 1 overlapping with that of the present TARN for comparison.

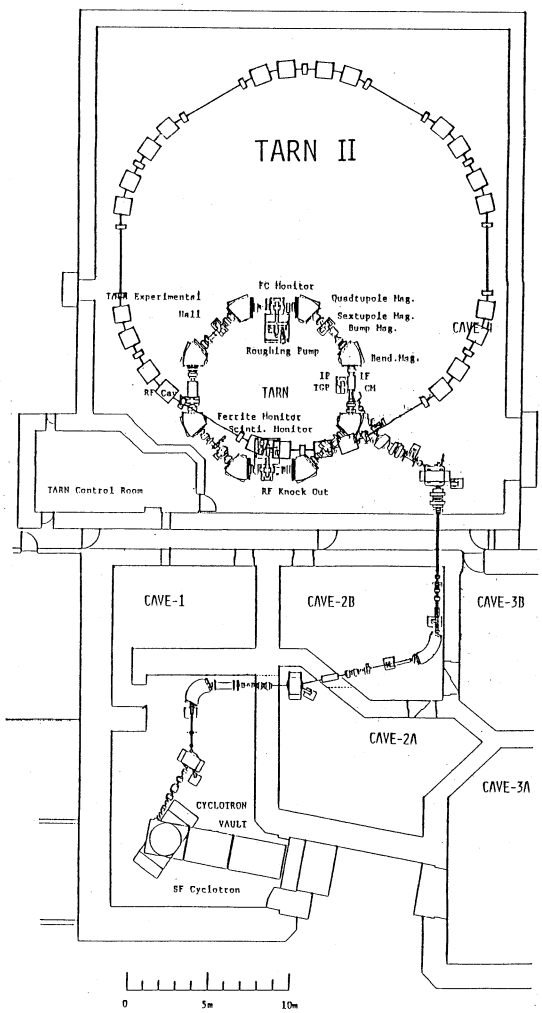

Fig. 1 Layout of TARN II.

Lattice Design

TARN II lattice is designed to be able to operate with two different excitation modes. One of which aims at large intensity multiplication and higher maximum energy attainable in the limited site (Synchrotron Mode). The other provides doubly achromatic long straight sections needed for cooler equipments so as to be free from the transverse emittance blow up due to momentum correction during the cooling process (Cooler Ring Mode).

The lattice is based on a simple FODO structure. With Synchrotron Mode, intensity increase of 20 times by the multi-turn injection into horizontal transverse phase space is assumed. So the maximum value of β_x is suppressed at rather smaller value (∿10 m) by taking higher superperiodicity of 6. In Fig. 2, beta and

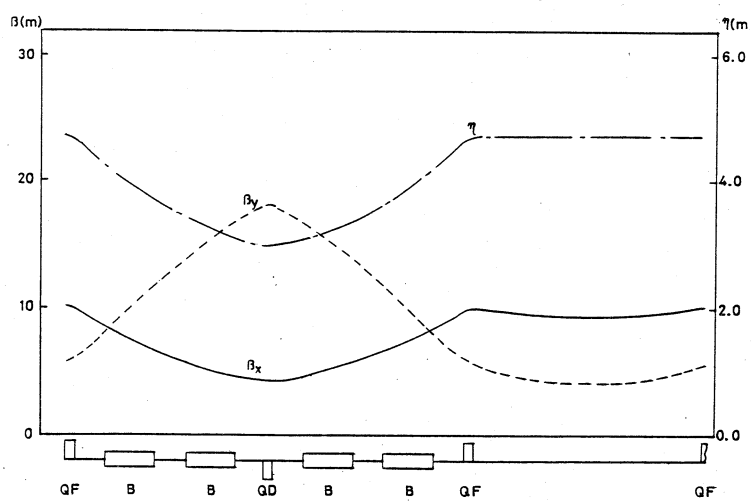

Fig. 2 Beta and dispersion functions of TARN II Synchrotron Mode. ν-values are chosen at around 1.75 both in horizontal and vertical directions.

Table 1

Magnetic focusing system of TARN II

Maximum Magnetic Rigidity		68.75 kG·m
Average Radius		12.03 m
Circumference		75.60 m
Radius of Curvature		3.82 m
Focusing Structure		FBDBFO
Repetition Rate		1/2 Hz
Maximum Field of Dipole Magnet		18 kG
Maximum Field Gradient of Quadrupole Magnet		70 kG/m
Number of Dipole Magnets		24
Number of Quadrupole Magnets		18
Length of Dipole Magnet		1.00 m
Length of Quadrupole Magnet		0.20 m
Superperiodicity		
Synchrotron Mode		6
Cooler Ring Mode		3
Transition Gamma		
Synchrotron Mode		1.86
Cooler Ring Mode		2.97
Betatron Tune Value	Horizontal	Vertical
Synchrotron Mode	∿ 1.75	∿ 1.75
Cooler Ring Mode	∿ 1.75	∿ 1.25

dispersion functions are shown for a unit cell, which is composed of a single FODO cell and a long straight section of 4 m in length. So the superperiod coincides with the unit cell, which is the same as the present TARN. ν-values are chosen at 1.75 both in horizontal and vertical directions.

For Cooler Ring Mode, long straight sections with large dispersion are also needed as well as doubly achromatic long straight section if an internal target experiment with cooled beam is considered. So the structure where every second long straight section is made doubly achromatic and other long straight sections have rather larger dispersion (∿5 m) is adopted. From the above condition, the constraints to be imposed on field gradients of quadrupole magnets are obtained by multiplication of transfer matrices. The arrangement of magnet elements is made symmetric with respect to the point B in Fig. 3. If we denote the transfer matrix from A to B by M which is written as

$$M = \begin{pmatrix} a & b & c \\ d & e & f \\ 0 & 0 & 1 \end{pmatrix} , \qquad (1)$$

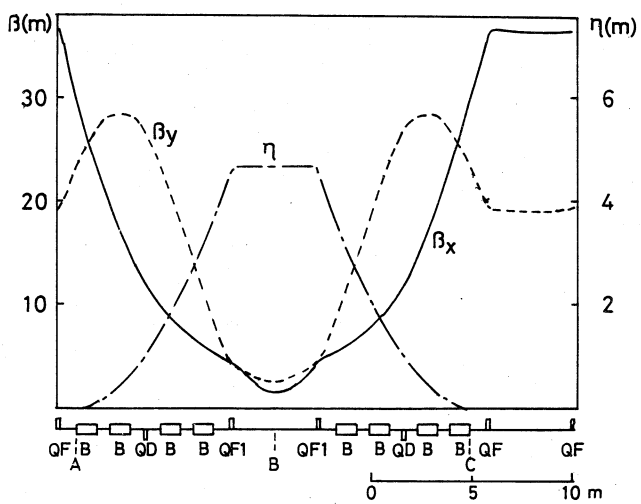

Fig. 3 Beta and dispersion functions of TARN II Cooler Ring Mode. ν-values are chosen at ∿1.75 and ∿1.25 for horizontal and vertical directions, respectively. One third of the circumference is shown in the figure.

the constraint to realize doubly achromatic long straight sections just outside of points A and C in Fig. 3 is given by[3]

$$f = 0 . \qquad (2)$$

The dispersion function at the point B , η_0, can be given by

$$\eta_0 = c . \qquad (3)$$

The numerical calculation of Twiss parameters and dispersion is executed with use of computer code SYNCH[4]. For the electron cooling section, rather smooth β-functions are preferable and low β is needed for the target position (point B). In Fig. 3, beta and dispersion functions of the Cooler Ring Mode are given for the unit cell for ν-values of 1.75 and 1.25 in horizontal and vertical directions, respectively. The superperiodicity of this mode is 3 and one third of the circumference is shown in Fig. 3.

In Table 1, main parameters of magnetic focusing system of TARN II are listed up.

Magnet Design

Main magnet system of the ring consists of 24 dipole and 18 quadrupole magnets. Assuming the beam emittances of 400 mm·mrad and 10 mm·mrad for horizontal and vertical directions respectively and fractional momentum spread of ±0.22 %, aperture requirement is calculated as given in Table 2 for Synchrotron Mode. Thus the good field regions with the size of 200 x 50 mm² and 185 x 60 mm² (Hori. x Vert.) are needed for dipole and quadrupole magnets, respectively. Due to the fact that maximum values of beta and dispersion functions are larger for Cooler Ring Mode, the horizontal emittance after multiturn injection should be limited below 70 mm·mrad for the case of Cooler Ring Mode. Because Cooler Ring Mode aims at high quality beam even if sacrificing beam intensity a little, this restriction can be tolerable. For this mode, vertical aperture with the size of ± 30 mm is required both in dipole and quadrupole magnets. So the gap of the dipole magnet is chosen at 80 mm considering additional spaces of vacuum chamber wall and heat insulator for baking process to attain ultra-high (∿ 10^{-11} Torr) vacuum.

The ring is to be AC excited by 1/2 Hz with rising time of 750 msec. So as to suppress the eddy current effect, the magnet should be made of stacked laminated steel. Quadrupole magnets in the present TARN are already made by laminated cores[5] and they are to be converted to the focusing elements in TARN II. Although several quadrupole magnets are to be made, their design is basically the same as that of the present TARN.

As the type of dipole magnet to be newly made, H-type is adopted. Window-frame type has the merit of good field homogeneity and compactness, but in this

Table 2

Aperture Requirement (Synchrotron Mode)

Horizontal Direction		
Source	in Dipole	in Quadrupole
Closed Orbit Displacement	14.9 mm	16.4 mm
Betatron Oscillation	58.1 mm	63.9 mm
Momentum Spread	8.9 mm	10.0 mm
Sagitta	16.4 mm	
Sum	98.3 mm	90.3 mm
Required Aperture (Half)	100 mm	92.5 mm

Vertical Direction		
Source	in Dipole	in Quadrupole
Closed Orbit Displacement	6.1 mm	6.4 mm
Betatron Oscillation	12.5 mm	13.0 mm
Sum	18.6 mm	19.4 mm
Required Aperture (Half)	25.0 mm	30.0 mm

type, coils are located where magnetic field is so high that relatively larger eddy current in the conductor of the coil is anticipated. C-type magnet is convenient for access to the vaccum chamber, but its size becomes considerably larger. The size of the H-type magnet is moderate and its coils are located at places with relatively lower magnetic field. Coils are shielded from the region of beam location by the pole for H- and C-type and the field structure is ,in general, insensitive to coil arrangement error. For H-type, reflection symmetry cocerning the center line in radial direction exists and quadrupole and octapole components are suppressed and only such component originated by fabrication error can appear, which is also the one reason H-type is superior to C-type.

The dipole magnet is decided to be made by straight shape for its easiness of fabrication and convenience for the case of further conversion to a larger ring. The magnet length is made rather short(1 m) to reduce the sagitta at reasonable value(16.4 mm).

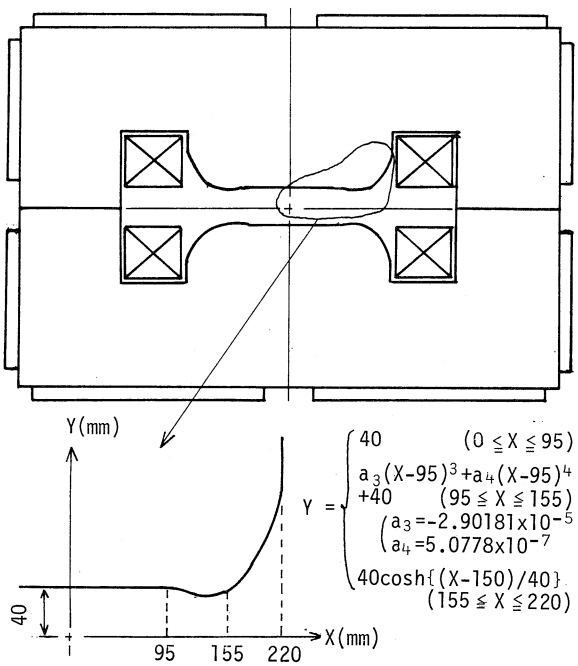

Fig. 4 Cross sectional view of the dipole magnet.

So as to realize the field uniformity in the wide range of ±100 mm and for wide range of excitation level up to 18 kG, the pole edge are shaped with B constant curve[6] as shown in Fig. 4. So as to modify the field strength which tends to fall down at both sides due to saturation of iron at high fields, small shims are attached at both sides which continues smoothly to the B constant curve as shown in Fig. 4. The shape of the shim is determined based on the result of computer calculation with use of TRIM[7].

As the material of laminated core, cold rolled silicon steel strip (S23) with special treatment is adopted. The thickness of the strip is 0.5 mm and its surface is coated by an inorganic insulation layer. Both ends of the magnet are cut by three steps[8] which approximate the Rogowski's curve[9], so as to suppress the variation of the effective boundary of the magnetic field depending on the excitation level. The overall view of the fabricated dipole magnet is shown in Fig. 5.

Field Measurement of the Dipole Magnet

The static field structure of the dipole magnet has been studied with the available DC power supply. A temperature controled Hall-probe (siemens FC 33) with a dimension of 3 x 6 mm² has been used for field mapping. It is position controlled with driving mechanism which utilize ball screws and pulse motors in horizontal plane[10]. The height of the probe can be changed

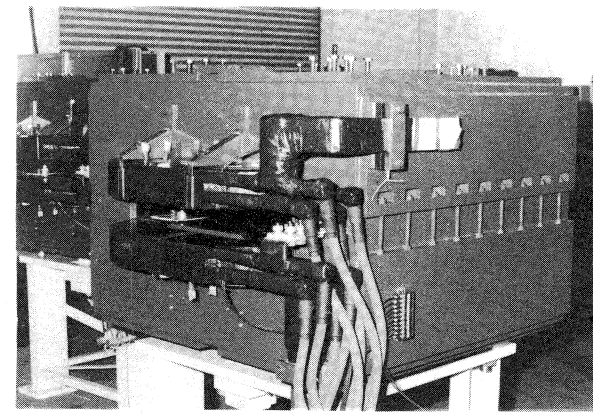

Fig. 5 Overall view of the new dipole magnet.

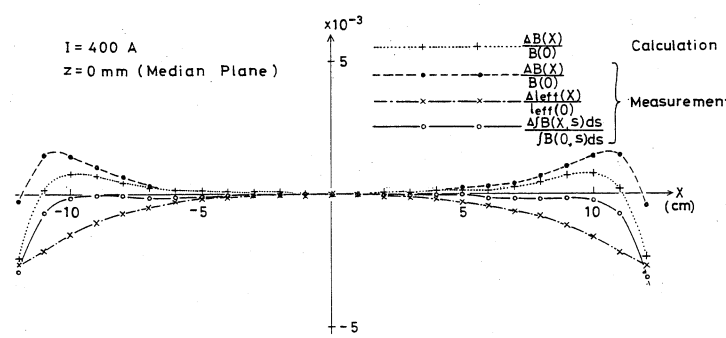

Fig. 6 Radial field distribution of the dipole magnet.

mannually. Data taking has been executed with a 16-bits microcomputer with CAMAC interface.

In Fig. 6, the measured field structure in radial direction is shown together with that of the computer calculation with TRIM. In the figure, also shown are measured structure of the effective length and integrated field strength (∫Bds). It is known from the figure, that good field region of ±100 mm is attained. The effect of shim can well cancell the variation of effective length.

The results above mentioned are only for lower magnetic field due to limitation of power supply. Magnet quality at higher field where saturation of iron appears and AC characteristics are to be evaluated after construction of the power supply for TARN II itself.

Acknowledgement

The authors would like to present their sincere thanks to Prof. Y. Hirao for his fruitful discussion and continuous encouragement throughout the work. Orbit calculation with SYNCH and field calculation with TRIM are performed with M-180-II AD at INS.

References

1) A. Noda, INS-KIKUCHI WINTER SCHOOL on Accelerators for Nuclear Physics, Genshikaku Kenkyu Vol. 28, No. 3 (1984) 367.
2) Y. Hirao et al., INS-NUMA-5 (1977).
3) A. Noda, Proc. of Workshop on "Electron Cooling and Beam Circulation", RCNP-T-12 (1983)3-1(in Japanese).
4) A. A. Garren and J. W. Eusebio, Lawrence Radiation Laboratory Report UCID-10154 (1965).
5) A. Noda et al., INS-NUMA-23 (1980).
6) H. Kumagai, Nucl. Instr. Meth. 6 (1960) 213.
7) A. M. Winslow, UCRL-7784 (1964).
8) A. Itano et al., Contribution to this symposium.
9) W. Rogowski, Archiv für Electrotechnik, 7 (1923) 1.
10) T. Hori et al., INS-NUMA-24.